1.3 **LIDAR based Measurements of Turbulent Dissipation above Urban Areas**

Marko Princevac[*1], PapaMagatte Diagne[1], and Ronald Calhoun[2]
[1]University of California, Riverside 92521
[2]Arizona State University, Tempe 85287

1. INTRODUCTION

From June 28 to July 31, 2003 the Joint Urban Atmospheric Dispersion Field Study took place in Oklahoma City, Oklahoma, USA. The purpose was to study the transport and dispersion of contaminants in urban environments. Knowledge gained from the study will be used to improve, refine and validate computer models that simulate flow in urban areas. Meteorological instrumentation and tracer samplers were installed at various locations in and around the city to provide detailed measurement of key meteorological variables and tracer gas concentrations. Teams from several National Laboratories and Universities deployed a barrage of instruments, including sonic anemometers, hygrometers, energy balance stations, temperature sensors, SODARs, RASS and two Doppler LIDARs for measurements of entire velocity fields. One LIDAR belongs to the Arizona State University and the other to the Army Research Laboratory. A detailed field campaign description is given in Allwine ***et al.*** 2004. This communication presents progress in using the structure function in conjunction with single radial velocity field measurements, from coherent Doppler-LIDAR, to measure turbulent dissipation. Turbulent dissipation is conventionally measured using hotwires or sonic anemometers utilizing the Kolmogorov -5/3 law for the inertial subrange. These both are point measurements limited to a small stationary control volume. A common way of measuring characteristics of turbulence, high above the ground, is through expensive airplane based measurements. On the contrary, LIDAR gives a three dimensional field of the radial velocity component within a range of several kilometers, is ground deployed and relatively cheap. In addition to the large range, LIDAR has a relatively high sampling frequency. In the presented case, the sampling frequency is 500 Hz and velocity data is subsequently averaged over 50 and 100 pulses giving the actual sampling rate of 10 and 5 Hz, respectively. This sampling frequency is fast enough for resolving the turbulence timescale. Here, we advance the idea of using LIDAR as a remote sensing instrument for the dissipation measurements above urban areas. Using the second-order structure function, a dissipation field is extracted from the radial velocity field. The radial velocity field is filtered to remove all data with the low signal to noise ratio (SNR). The filtering is applied individually to each range-gate over the entire time interval of measurement. For this analysis a simple stare scan from ASU LIDAR is used (Figure 1).

Figure 1. Oklahoma City – Central Business District, as seen from the ASU LIDAR location. The red dot marks the location of the LIDAR beam passing above and between the buildings.

2. MEASUREMENTS AND DATA DENOISING

The LIDARs were designed by Coherent Tech. Inc. and utilize a 2 μm wavelength laser. The 2 μm laser is eye safe and, since velocity scales linearly with the operating wavelength (Frehlich and Yadlowsky 1994), performs better than the 10 μm LIDAR. Measured radial velocity in range gate 1 (400 m from the LIDAR) is given Figure 2. Figures 3 and 4 present the radial velocity measured in range gate 40 (2700 m from the LIDAR) and 80 (5200 m from the LIDAR), respectively. The sampling rate was 10 Hz. Weakening of the signal quality (increase in noise) with increased distance is evident. The level of noise in range gates far away from the LIDAR was so high that it completely mutilated the

[*]Corresponding author address: Marko Princevac, University of California, Department for Mechanical Engineering, Riverside, CA 92507. Email: marko@engr.ucr.edu

measurement making further data analysis questionable.

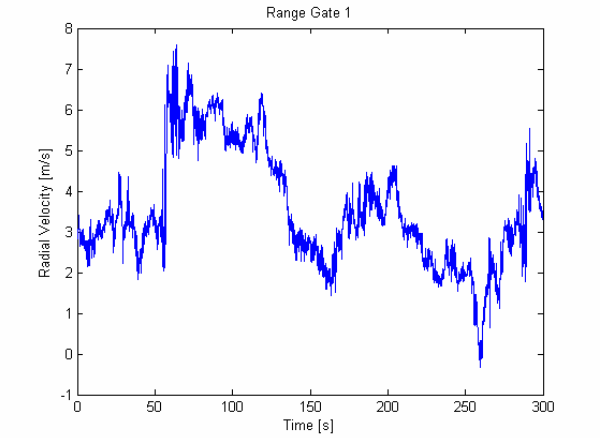

Figure 2. The time series of radial wind velocity component from the Range Gate 1.

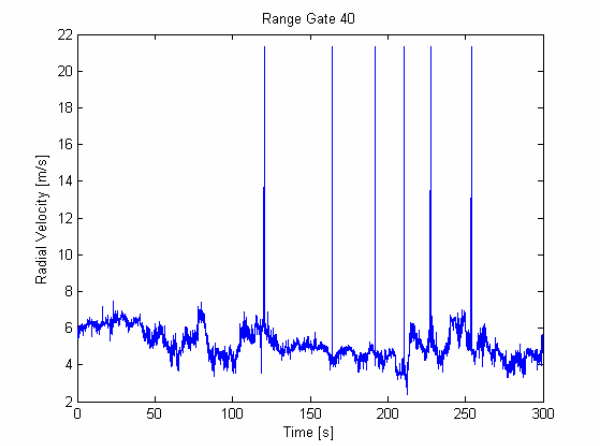

Figure 3. The time series of radial wind velocity component from the Range Gate 40. The velocity peaks caused by the random noise can be seen.

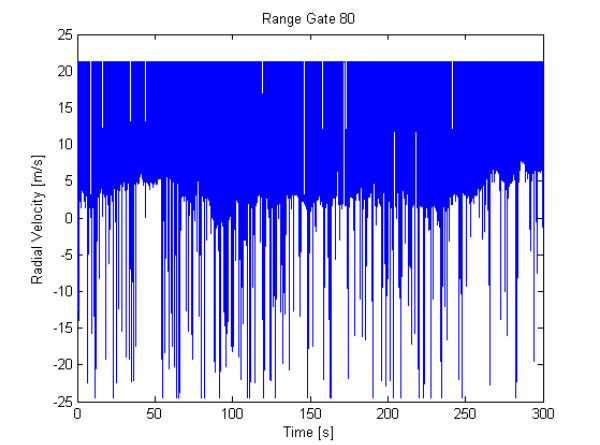

Figure 4. The time series of radial wind velocity component from the Range Gate 80. High noise level radically alters the measurements.

These high levels of noise required rigorous data filtering prior to analysis. The averaged signal to noise ratio (SNR) together with *rms* value is given in Figure 5.

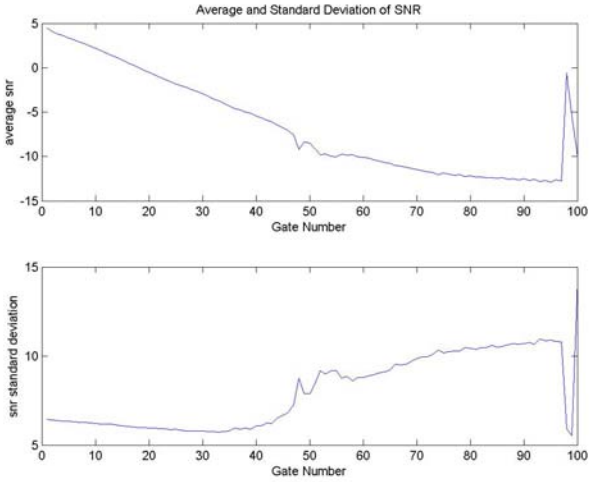

Figure 5. Averages of SNR and SNR's standard deviation vs. Gate number. These values are averaged over one hour.

To prepare data for the analysis, the following two-step filtering was used. First step was utilizing the SNR data to determine bad points. After experimenting with several different values, *SNR = -5* was selected as a lower threshold for acceptable data. All data points whose SNR was below -5 were replaced with the median value of the closest 20 data points with SNR > -5. Clearly (see Figure 5), this way of filtering left data from range gate 50 and higher still questionable. SNR-filtered velocities are presented in figures 6 and 7 for range rates 40 and 80, respectively.

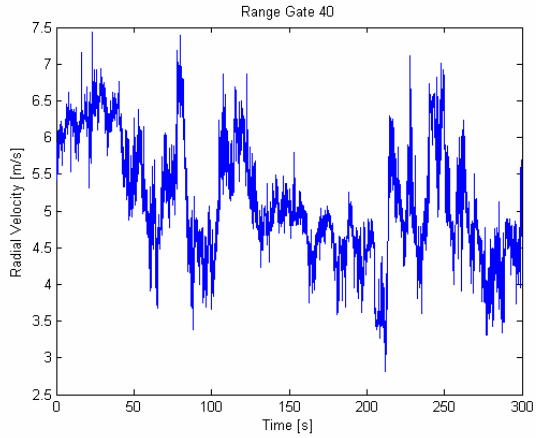

Figure 6. The time series of SNR-filtered radial wind velocity component from the Range Gate 40. Compare to Figure 3.

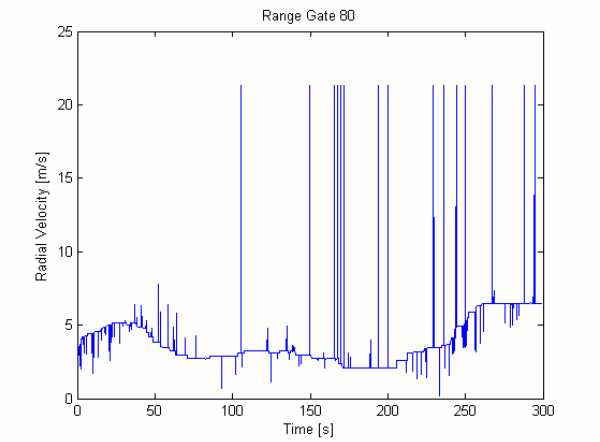

Figure 6. The time series of SNR-filtered radial wind velocity component from the Range Gate 80. Compare to Figure 4.

One may conclude that the velocity in the range gate 40 does not require further filtering. However, this is not the case for range gate 80. The second filtering step is based on the relative jump of the velocity value compared to the previous and following data point. If this jump is more than a threshold value in any direction, the data point is replaced with the median value of the closest 20 data points whose velocity is within the threshold value from the median velocity of the observed gate. By careful data examination and after trying several threshold values, the threshold of 5 m/s was adopted.

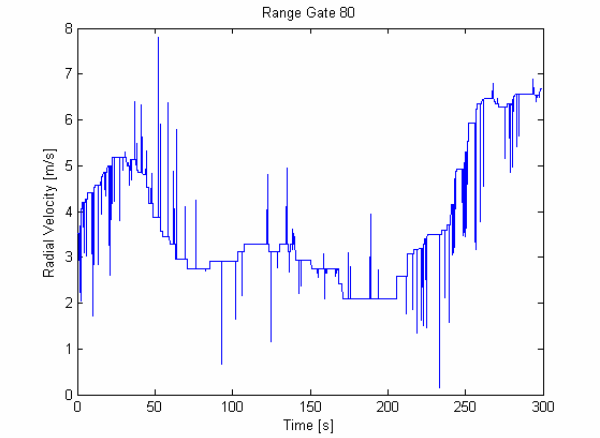

Figure 7. The time series of two-step filtered radial wind velocity component from the Range Gate 80. Compare to figures 4 and 6.

Final data, as seen in Figure 7, gives a good idea of the general velocity trend, however this data cannot be used for analysis which requires high frequency data. Due to the high volume of bad and questionable data points, most of the information on fast fluctuations is removed together with these data points. Due to the higher data quality in the first 40 range gates, higher range gates were not used in the following analysis.

3. DATA ANALYSIS

After filtering the data, the second order structure function (*m=2*) is calculated according to the definition

$$S_m(r) = < [u(x+r,t) - u(x,t)]^m >, \qquad (1)$$

where *u* represents the radial velocity fluctuation, *x* is gate location with respect to the LIDAR, *t* is time and *r* is the distance between gates. Using dimensional arguments (Monin and Yaglom 1975), this structure function can be expressed as

$$S_2(r) = C_V \varepsilon^{2/3} r^{2/3} \qquad (2)$$

where $C_v \approx 2$ is the Kolmogorov constant and ε is the energy dissipation rate. The structure function calculated from gates 1 to 40 is given in Figure 8.

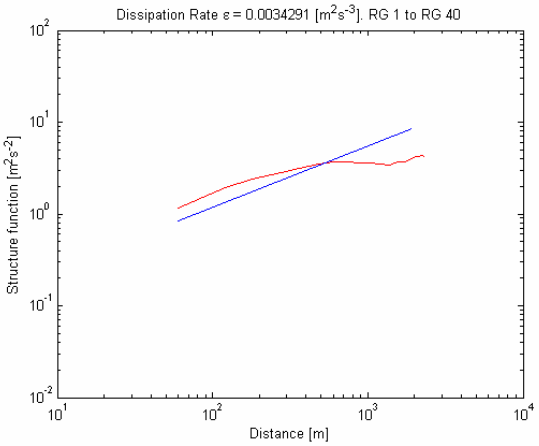

Figure 8. The structure function calculated from gates 1 through 40.

The straight blue line in Figure 8 presents the best fit of Equation 2 to the calculated structure function. This best fit is obtained by setting the energy dissipation rate ε equal to 0.0034 [m^2s^{-3}].

Figure 9 gives the structure function calculated using only the closest 20 range gates to the LIDAR. These range gates are approximately 1 km upstream from the urban core and it is not expected that they may in any way be influenced by the urban core.

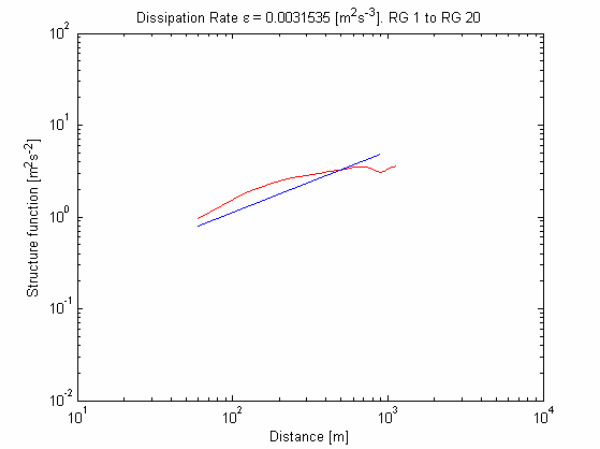

Figure 9. The structure function calculated from gates 1 through 20.

In the same way as in Figure 8, the blue line in Figure 9 presents the calculated structure function fitted to Equation 2. This best fit is obtained by setting the energy dissipation rate ε equal to 0.0031 [m^2s^{-3}]. This may be considered the free stream dissipation since it is not in the vicinity of any obstacles. Figure 10 gives the structure function calculated from the range gates in the urban vicinity.

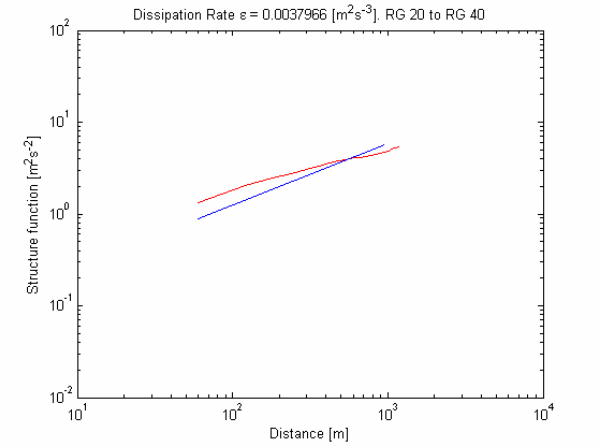

Figure 10. The structure function calculated from gates 20 through 40.

The best fit of Equation 2 to the structure function presented in the figure 10 gives the energy dissipation rate ε to be 0.0037 [m^2s^{-3}].

In the summary we may say that the turbulent energy dissipation estimate corroborate with previous work (Frehlich *et al.* 1998). Measured dissipation varies around 0.0035 [m^2/s^{-3}] depending on the distance from the LIDAR and probably the vicinity of the urban core. At this stage, due to the noisy data, the results obtained for the urban vicinity should be taken with caution. Another uncertainty in this analysis is the Kolmogorov constant C_v. Here it is assumed that C_v=2, however many investigations (e.g. Sreenivasan, 1995) suggest that the Kolmogorov constant may not be constant at all and can vary in the range from 1.8 to 2.6.

4. REFERENCES

Allwine, K.J., M.J. Leach, L. W. Stockham, J.S. Shinn, R. P. Hosker, J.F. Bowers, and J.C. Pace: Overview of Joint Urban 2003 – An atmospheric dispersion study in Oklahoma City, American Meteorological Society, *84th AMS annual meeting* 2003, January 2004, Seittle, WA.

Frehlich, R. and M. J. Yadlowsky: Performance of mean-frequency estimators for Doppler radar and lidar. *J. Atmos. Oceanic Technol.*, **5**, 1217-1230, 1994.

Frehlich, R., S.M. Hannon, and S.W. Henderson: Coherent Doppler LIDAR measurements of Wind Field Statistics, *Bound. Layer. Meteo.*, **86**, 233-256, 1998.

Monin, A. S. and A. M. Yaglom.: 1975, *Statistical Fluid Mechanics: Mechanics of Turbulence*, Volume 2, MIT Press, 874 pp.

Sreenivasan, K.: On the universality of the Kolmogorov constant, *Phys. Fluids*, 7(11), 2778-2784, 1995